

Reversible polarization control of single photon emission

Robert J. Moerland*

Optical Sciences group, Faculty of Science & Technology and
MESA+ Institute for Nanotechnology,
University of Twente,
P.O. Box 217, NL-7500AE Enschede, the Netherlands

Tim H. Taminiau

ICFO-Institut de Ciències Fòniques,
Mediterranean Technology Park,
08860 Castelldefels (Barcelona), Spain

Lukas Novotny

The Institute of Optics, University of Rochester,
Rochester NY 14627, USA

Niek F. van Hulst

ICFO-Institut de Ciències Fòniques,
Mediterranean Technology Park,
08860 Castelldefels (Barcelona), Spain

Laurens Kuipers[†]

FOM Institute for Atomic and Molecular Physics (AMOLF)

Kruislaan 407, NL-1098SJ, Amsterdam, The Netherlands

September 24, 2007

*r.moerland@utwente.nl

†l.kuipers@amolf.nl

Abstract

We present a method that allows reversible and a-priori control of the polarization of a photon emitted by a single molecule by introducing a nanoscale metal object in its near field. It is experimentally shown that, with the metal close to the emitter, the polarization ratio of the emission can be varied by a factor of 2. The tunability of polarization decays, when the metal is displaced by typically 30 nm. Calculations based on the multiple multipole method agree well with our experiments and predict even further enhancement with a suitable antenna design.

Spontaneous emission of single quantum systems, such as organic molecules and quantum dots, is finding widespread application in sensing and nanoscale imaging of (bio)chemical systems.^{1,2} The well defined photon statistics is explored for quantum information applications.^{3,4} Control over the photodynamics and polarization of single emitters would provide photons on demand with a chosen polarization. Indeed, manipulation of radiative decay is being studied by placing (single) emitters in photonic crystals,⁵ dielectric nanospheres^{6,7} and near metal structures.⁸⁻¹² It is well known that breaking symmetry with finite-sized nano-objects may lead to deviations of spontaneous emission properties of the emitter such as changes in lifetime¹³⁻¹⁵ and radiation pattern.^{16,17} With various scanning probe methods, employing e.g. aperture probes and metallic spheres, different groups have observed the dependence of fluorescence life time on the probe-molecule distance and the probe-sample separation.^{10,11,18,19} Furthermore, among e.g. quantum dots and NV-centers in diamond, single molecules are good candidates to be used as single-photon sources.⁴ By structuring the molecule's surroundings, e.g. with a photonic crystal or microcavity, the photons will be emitted into the mode dictated by the local environment.^{5,21} However, dynamic and reversible control of the polarization of the emission on a per-photon base has proven to be difficult, since this involves dynamically and

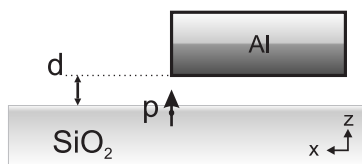


Figure 1: Principle for polarization control on the single emitter level. An aluminum disk ($\varepsilon = -38.4 + 10.2i$), 110 nm in diameter and 40 nm high, is placed near an embedded dipole \mathbf{p} at $d = 20$ nm. The dipole is situated 1 nm below the dielectric interface. By changing the position of the disk, the polarization of photons, radiated by the dipole, is changed.

controllably changing the molecule's nano-environment. Therefore, usually once a mode has been set for the molecule to emit into, it cannot be changed. In this Letter, we show a-priori control, and reversible change of, the polarization of the emitted light of a single molecule by manipulating the local environment of the molecule with a nanoscale object. Verified by experimental results, we present a theoretical three-dimensional model system that quantifies our proposed method.

The method is depicted schematically in Fig. 1. An emitter, e.g., a molecule, is embedded at 1 nm depth in a transparent substrate ($\varepsilon = 2.5$) with a transition dipole perpendicular to the substrate-air interface. The emitter is placed near a nanoscale metal object, in this case an aluminum disk ($\varepsilon = -38.4 + 10.2i$) of 110 nm diameter and 40 nm height to modify the environment of the radiating dipole. The disk is placed at a height of $d = 20$ nm above the surface. Fig. 1 depicts the particular configuration when the dipole is located right underneath the edge of the disk. We calculate the local electric field distribution by use of the multiple multipole (MMP) method.¹⁶ In the calculation, the radiation is 'collected' with a high-NA objective positioned in the $-z$ half-space, with its optical axis aligned to the z -axis. For this situation we calculate the x -polarized and y -polarized intensity distributions in the back focal plane of the objective. For a z -oriented dipole, having no objects in its near field, one expects an emis-

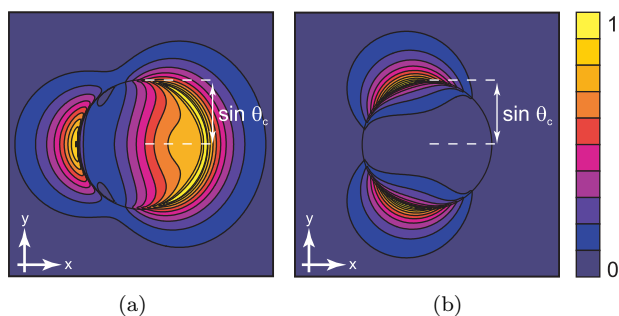


Figure 2: Calculated radiation patterns of a single molecule located underneath the edge of an aluminum disk (c.f. Fig. 1). The patterns correspond to the polarized intensity distributions in the back-focal plane of the collection objective. The circles indicate the critical angle of total internal reflection: $\theta_c = 41^\circ$. The molecule has its emission dipole in the z direction. (a) polarization in x direction; (b) polarization in y direction. The metal object influences the dipole's emission, inducing an in-plane component perpendicular to the nearest vertical edge of the disk. This effectively increases the polarization component perpendicular to the edge (arbitrary units, linear scaling, same scale in both figures).

sion pattern that has a cylindrical symmetry.²² Consequently, the polarization of the emission in the back focal plane of the objective is equally partitioned in x -polarized and y -polarized radiation (i.e., radial polarization). If the metal object is introduced into the near field, it modifies both the emission pattern and the polarization. The results for a configuration as in Fig. 1 are depicted in Fig. 2(a) and (b). We find that the metal edge influences the dipole's emission, inducing an in-plane component perpendicular to the vertical edge of the disk. This effectively increases the polarization component perpendicular to the metal edge (Fig. 2(a)). At the same time, polarization components parallel to the metal edge are suppressed (Fig. 2(b)). The influence on the polarization is maximal for this dipole orientation, since an in-plane orientation of the dipole will bias the polarization of the radiation in a certain direction which makes the relative change of the polarization direction smaller.

For our experiments, we use a home-built NSOM, see Fig. 3. Light from

an Argon-Krypton laser ($\lambda = 514$ nm, Ar⁺ line) is coupled into a focused ion beam (FIB) modified near-field fiber probe coated with aluminum.²³ This probe is used both to excite molecules in the sample and to control the polarization of their emission. As such, the role of the aluminum disk in Fig. 1 is performed by the sharp metal-glass transition at the edge of the aperture. The distance between the sample and the probe is controlled using shear-force feedback. When engaged, the shear-force feedback results in a probe-substrate distance of 20 - 25 nm.²⁴ With a piezo x - y - z driver we control the position of the molecule relative to the metal rim. The light emitted by the molecule is collected using a 1.3 NA oil-immersion objective. A long-pass filter blocks the excitation light coming from the probe. Finally, we probe the projected polarization state of the single emitter emission using a polarizing beam-splitter.^{25,26} The x - and y -polarized radiation is independently measured using avalanche photo diodes (APD x and APD y , respectively). Samples are prepared by dissolving 0.5% poly(methylmethacrylate) (PMMA) in toluene and adding carbocyanine (DiIC₁₈, $\lambda_{em,peak} = 570$ nm) dye molecules to a 10^{-8} molar concentration. This solution is spin-coated on plasma-etched glass substrates, resulting in a thin polymer matrix containing embedded DiIC₁₈ molecules. The samples are dried in air at room temperature. This procedure results in a polymer matrix with dispersed single molecules, fixed in position and orientation on the time scale of the experiment.¹⁷

The molecules are excited by the near field at the aperture of the probe, using circularly polarized incident light. By raster scanning the probe over the sample, the amount of photons detected by each APD as a function of probe position is obtained. The scan yields an image map containing the locations of each molecule and the projected polarization state of the emitted light at each position of the probe. A typical image is shown in Fig. 4. Here, the

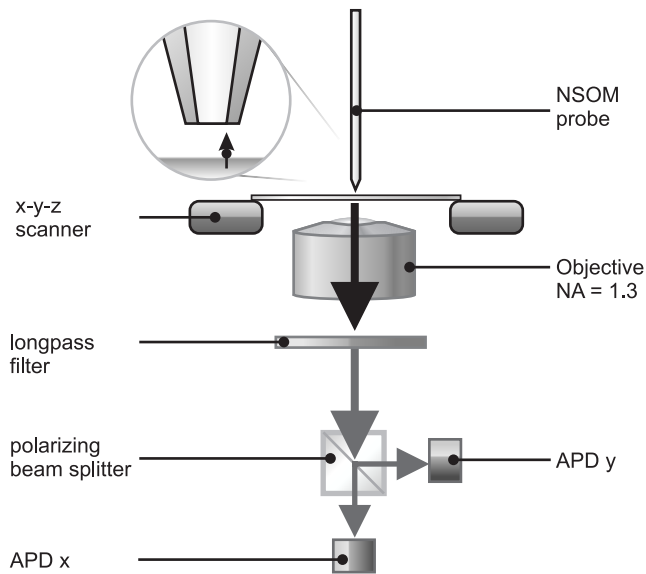


Figure 3: Schematic depiction of the experimental setup. Light from an Ar-Kr laser (not shown) is coupled into the near-field probe. Fluorescence, emitted by single molecules in the sample, is collected by an objective (NA 1.3) and separated from the laser light by a long pass filter. A polarizing beam splitter divides the radiation into its two orthogonal polarization components which are detected with APD x and APD y , respectively. The inset show a schematic cross-section of an aperture probe nearby a z -oriented molecule. The sharp glass-metal edge is used to influence the polarization of the emission of the molecule.

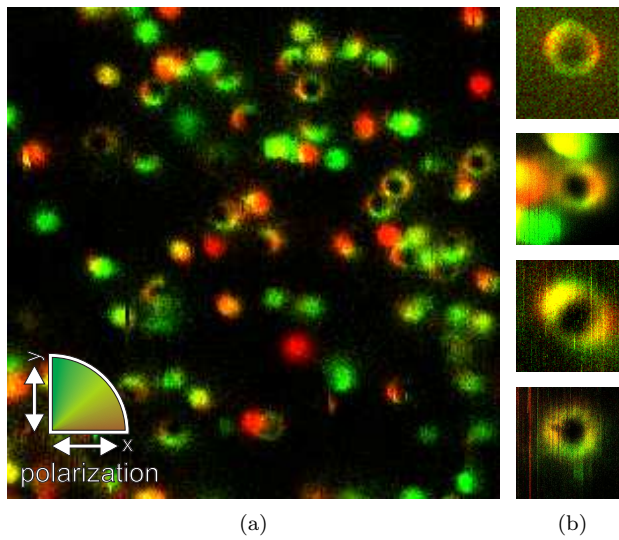


Figure 4: (a) Single molecule polarization map obtained by raster scanning the near-field probe over the surface of the sample. Rings, the result of the interaction of the z -oriented field from the probe with z -oriented molecules, can clearly be distinguished from the in-plane oriented molecules which are represented by the colored spots. The polarization is color coded, $x = \text{red}$, $y = \text{green}$ — see inset. Excitation wavelength: 514 nm. Scan area: $3 \times 3 \mu\text{m}$. (b) Close-up of four different z -oriented molecules measured with different probes. The change in color of the ring around the perimeter and thus the change in degree of polarization of the emission radiated by the molecule, as a function of probe position, is evident. Scan area: $500 \times 500 \text{ nm}$.

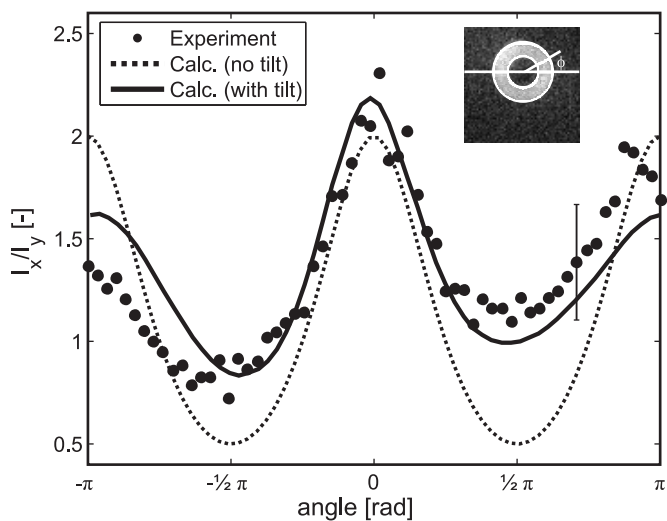


Figure 5: Polarization ratio I_x/I_y as a function of the angle ϕ for a z -oriented molecule. The inset shows an image of the obtained molecule map. Data from the area between the white circles are integrated radially and plotted as circles (typical error bar shown for one data point, others left out for clarity). As the relative position of the metal probe changes, the polarization ratio of the emitted photons changes. A maximum I_x/I_y of 2 is found. For $A(r, d) = 2.4$ and $B(r, d) = 1.2$ (see main text), the dotted curve is obtained. The data exhibits a good qualitative correspondence to this calculation. Taking probe tilt into account, together with a small bias due to an inclination of the molecule's dipole, an even better correspondence is obtained (solid curve).

following color-coding method is used: the signal from APD x is displayed in red, the signal from APD y is displayed in green. Clearly visible amongst all the in-plane oriented molecules, which show up as colored filled spots, are ring-shaped patterns. These excitation patterns are the result of fluorescence of z -oriented molecules that are only excited by an E-field in the z direction, which is only found at the rim of the aperture.^{27–30} A close-up of four individual molecules, each from a different sample and measured with different probes, is shown in Fig. 4(b). These close-ups show that the degree of polarization is *reversibly* altered while scanning the probe over the molecule, as is evident from the change of color around the perimeter of the ring-shaped pattern.

The experimental results therefore prove that the polarization of the emitted photons can be reversibly influenced with a metal nanostructure in close proximity. Because of the axial symmetry of the aperture, the intensity of the measured x -polarized radiation I_x can be written as

$$I_x(r, d, \phi) = A(r, d) \cos^2(\phi) + B(r, d) \sin^2(\phi) \quad (1)$$

where r is the in-plane probe-molecule separation, d is the probe-surface separation, ϕ is the azimuthal angle and $A(r, d)$ and $B(r, d)$ are functions that contain the excitation efficiency and the radiative properties of the molecule. For the y -polarized radiation, $A(r, d)$ and $B(r, d)$ are interchanged, assuming perfect symmetry. Thus, an induced polarization anisotropy at a given azimuthal angle ϕ , will result in a periodic modulation of the anisotropy as a function of ϕ .

The polarization ratio of the fluorescence is defined as I_x/I_y , where I_x and I_y are the number of photons measured by APD x and APD y , respectively. We can quantify the measured polarization ratio as a function of angle for a single molecule, which is shown in Fig. 5. The polarization ratio of the photon emission indeed changes as the molecule's relative position moves around the perimeter of the probe. The measured polarization ratio goes up to a factor of slightly more than 2, for $\phi = 0$. From the MMP calculation we find that $I_x/I_y = 2$ for $A(r, d) = 2.4$ and $B(r, d) = 1.2$, at $d = 22$ nm. The resulting calculated I_x/I_y is shown as a dotted curve (Fig. 5). The qualitative correspondence of the measured polarization change and the calculation is clearly visible. The increasing trend of I_x/I_y from $\phi = -\pi$ to $\phi = +\pi$ however cannot be explained with eq. 1. The measurements can be reproduced by incorporating the distance dependence of $A(r, d)$ and $B(r, d)$ and correcting for a slight tilt of the tip with respect to the surface sample. Additionally, a small tilt of the molecule's dipole can result in a bias towards a polarization state of the emission. Consequently,

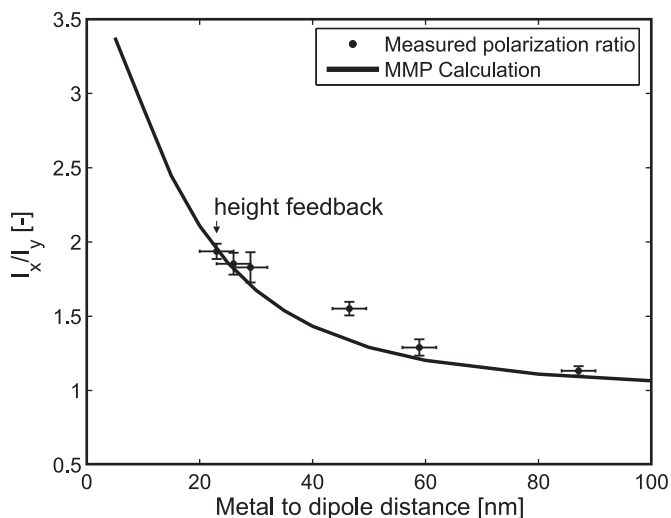


Figure 6: (color online) Polarization ratio as a function of distance. The measured polarization ratio goes up to a factor of 2 for the engaged height feedback. The rapid drop within 30–40 nm to values near unity — the limit value for an unperturbed molecule — reveals that the molecule is influenced only in the near field.

a fit of a tilt angle of 9° , plus a bias of 16% of the total collected power towards the x -polarization yields an improved correspondence between experiment and calculation (solid curve in Fig. 5). According to the tilted tip model, the tip is then closest to the surface at an azimuthal angle of $\phi = 0.18\pi$ with a gap width of 21 nm. We still notice a minor asymmetry in the position of the maxima in Fig 5, which we attribute to small imperfections of the probe.

In our experiments we have obtained, with the same probe used to obtain the data in Fig. 6, the degree of polarization control as a function of gap width, i.e. the height of the probe above the molecule. To enhance signal to noise, the polarization ratio is determined by integrating I_x/I_y from $\phi = -0.13\pi$ and $\phi = 0.13\pi$ c.f. Fig 5. The values obtained are plotted in the graph shown in Fig. 6. The absolute height, corresponding to an engaged shear-force feedback, was set to 23 nm as found before from the model incorporating tip tilt. This distance

indeed corresponds to typical shear-force feedback distances.²⁴ The following points can be observed: the measured ratio I_x/I_y for small distances, e.g. for the engaged feedback tip-surface distance, is approximately 2. Furthermore, the fact that the polarization ratio rapidly decays when the separation between the probe and the molecule is increased by only 30–40 nm, reveals that the influence of the metal is a true near-field effect. Finally, for probe-molecule distances that are ‘far’ away, the polarization ratio goes to unity, which can be expected for a z -oriented single dipole in stratified media without any objects in its near field. A full three-dimensional MMP calculation, shown in Fig. 6 as a black curve, confirms the observed behavior. Additionally, this calculation indicates that even better control can readily be obtained by further decreasing the distance between the emitter and the metal. We note that, despite the fact that in the experiment a ring-like structure (the probe) was used instead of a metal disk, the experiments and calculations match quite well. We believe that this is due to the fact that, since the aperture of the probe used in this experiment is 130 nm in diameter, the influence of the metal edge that is not right above the molecule is negligible. Moreover, we do not expect a sharp resonances for the the metal disk or the probe geometry, which would alter the outcome of the experiment completely.

In summary, we have shown in experiment and by calculation that the polarization of single photon emission can be changed and reversibly controlled. The control is achieved by placing a metal nanoscale object, in the form of the sharp glass-metal edge of an aperture-type probe, into the near field of a single molecule. Experimentally, a polarization anisotropy of a factor of 2 is induced. The rapid decay of the polarization anisotropy with distance shows that the control is strongly dependent on the interaction of the near field of the dipole with the metal probe. Both experiments and calculations for the given

control scheme show that the degree of polarization is altered in favor of the polarization component parallel to the dielectric interface and perpendicular to the closest vertical metal edge of the aluminum probe. Our calculations predict that a factor of 3 of polarization anisotropy should well be possible by placing the metal objects closer to the emitter. Even stronger emission control is expected for resonant structures which exhibit enhanced localized fields and are in resonance with the molecule.³¹

This work is part of the research program of the Stichting voor Fundamenteel Onderzoek der Materie (FOM), which is financially supported by the Nederlandse Organisatie voor Wetenschappelijk Onderzoek (NWO) and by the Petroleum Research Foundation (grant PRF 42545-AC10).

References

1. Y. Lill, K. L. Martinez, M. A. Lill, B. H. Meyer, H. Vogel, and B. Hecht. Kinetics of the initial steps of G protein-coupled receptor-mediated cellular signaling revealed by single-molecule imaging. *Chemphyschem*, 6(8):1633–1640, 2005.
2. A. Friedrich, J. D. Hoheisel, N. Marme, and J. P. Knemeyer. Dna-probes for the highly sensitive identification of single nucleotide polymorphism using single-molecule spectroscopy. *Febs Lett.*, 581(8):1644–1648, 2007.
3. W. E. Moerner. Single-photon sources based on single molecules in solids. *New J. Phys.*, 6:88, 2004.
4. C. Brunel, B. Lounis, P. Tamarat, and M. Orrit. Triggered source of single photons based on controlled single molecule fluorescence. *Phys. Rev. Lett.*, 83(14):2722–2725, 1999.

5. P. Lodahl, A. F. van Driel, I. S. Nikolaev, A. Irman, K. Overgaag, D. L. Vanmaekelbergh, and W. L. Vos. Controlling the dynamics of spontaneous emission from quantum dots by photonic crystals. *Nature*, 430:654–657, 2004.
6. M. D. Barnes, C. Y. Kung, W. B. Whitten, J. M. Ramsey, S. Arnold, and S. Holler. Fluorescence of oriented molecules in a microcavity. *Phys. Rev. Lett.*, 76:3931–3934, 1996.
7. Hannes Schniepp and Vahid Sandoghdar. Spontaneous emission of europium ions embedded in dielectric nanospheres. *Phys. Rev. Lett.*, 89(25):257403, 2002.
8. K. H. Drexhage. *Prog. Opt.*, 12:163, 1974.
9. M. Steiner, F. Schleifenbaum, C. Stupperich, A. V. Failla, A. Hartschuh, and A. J. Meixner. Microcavity-controlled single-molecule fluorescence. *Chemphyschem*, 6(10):2190–2196, 2005.
10. S. Kuhn, U. Hakanson, L. Rogobete, and V. Sandoghdar. Enhancement of single-molecule fluorescence using a gold nanoparticle as an optical nanoantenna. *Phys. Rev. Lett.*, 97(1):017402, 2006.
11. P. Anger, P. Bharadwaj, and L. Novotny. Enhancement and quenching of single-molecule fluorescence. *Phys. Rev. Lett.*, 96(11):113002, 2006.
12. F. Tam, G. P. Goodrich, B. R. Johnson, and N. J. Halas. Plasmonic enhancement of molecular fluorescence. *Nano Lett.*, 7(2):496–501, 2007.
13. W. P. Ambrose, P. M. Goodwin, J. C. Martin, and R. A. Keller. Alterations of single-molecule fluorescence lifetimes in near-field optical microscopy. *Science*, 265:364–367, 1994.

14. Randy X. Bian, Robert C. Dunn, X. Sunney Xie, and P. T. Leung. Single molecule emission characteristics in near-field microscopy. *Phys. Rev. Lett.*, 75(26):4772–4775, Dec 1995.
15. Christian Girard, Olivier J. F. Martin, and Alain Dereux. Molecular life-time changes induced by nanometer scale optical fields. *Phys. Rev. Lett.*, 75(17):3098–3101, Oct 1995.
16. L. Novotny. Single molecule fluorescence in inhomogeneous environments. *Appl. Phys. Lett.*, 69:3806–3808, 1996.
17. H. Gersen, M. F. Garcia-Parajo, L. Novotny, J. A. Veerman, L. Kuipers, and N. F. van Hulst. Influencing the angular emission of a single molecule. *Phys. Rev. Lett.*, 85:5312–5315, 2000.
18. X. S. Xie and R. C. Dunn. Probing single-molecule dynamics. *Science*, 265:361–364, 1994.
19. J. K. Trautman and J. J. Macklin. Time-resolved spectroscopy of single molecules using near-field and far-field optics. *Chem. Phys.*, 205:221–229, 1996.
20. F. Jelezko, T. Gaebel, I. Popa, M. Domhan, A. Gruber, and J. Wrachtrup. Observation of coherent oscillation of a single nuclear spin and realization of a two-qubit conditional quantum gate. *Phys. Rev. Lett.*, 93(13):130501, 2004.
21. E. Moreau, I. Robert, J. M. Gerard, I. Abram, L. Manin, and V. Thierry-Mieg. Single-mode solid-state single photon source based on isolated quantum dots in pillar microcavities. *Appl. Phys. Lett.*, 79(18):2865–2867, 2001.
22. G. W. Ford and W. H. Weber. Electromagnetic interactions of molecules with metal surfaces. *Physics Reports*, 113(4):195–287, November 1984.

23. J. A. Veerman, A. M. Otter, L. Kuipers, and N. F. van Hulst. High definition aperture probes for near-field optical microscopy fabricated by focused ion beam milling. *Appl. Phys. Lett.*, 72:3115–3117, 1998.
24. K. Karrai and R. D. Grober. Piezoelectric tip-sample distance control for near-field optical microscopes. *Appl. Phys. Lett.*, 66:1842–1844, 1995.
25. K. G. Lee, H. W. Kihm, J. E. Kihm, W. J. Choi, H. Kim, C. Ropers, D. J. Park, Y. C. Yoon, S. B. Choi, H. Woo, J. Kim, B. Lee, Q. H. Park, C. Lienau, and D. S. Kim. Vector field microscopic imaging of light. *Nature Photonics*, 1(1):53–56, 2007.
26. H. Gersen, L. Novotny, L. Kuipers, and N. F. van Hulst. On the concept of imaging nanoscale vector fields. *Nature Photonics*, 1(5):242–242, 2007.
27. E. Betzig and R. J. Chichester. Single molecules observed by near-field scanning optical microscopy. *Science*, 262:1422–1425, 1993.
28. J. A. Veerman, M. F. Garcia-Parajo, L. Kuipers, and N. F. van Hulst. Single molecule mapping of the optical field distribution of probes for near-field microscopy. *J. Microscopy-Oxford*, 194:477–482, 1999.
29. B. Sick, B. Hecht, U. P. Wild, and L. Novotny. Probing confined fields with single molecules and vice versa. *J. Microscopy-Oxford*, 202:365–373, 2001.
30. R. J. Moerland, N. F. van Hulst, H. Gersen, and L. Kuipers. Probing the negative permittivity perfect lens at optical frequencies using near-field optics and single molecule detection. *Optics Express*, 13(5):1604 – 1614, 2005.
31. T.H. Taminiau, R.J. Moerland, F.B. Segerink, L. Kuipers, and N.F. van Hulst. $\lambda/4$ resonance of an optical monopole antenna probed by single molecule fluorescence. *Nano Letters*, 7(1):28–33, 2007.